Influence of Stoichiometry and Alkalinity on Barium Hexaferrite Formation via the Supercritical Water Crystallization Method

Seungwook Rho and Sangdo Park*

Energy and Environment Research Department, Korea Institute of Energy Research,
P.O. Box 103, Yoosung, Daejeon 305-600, Korea

Abstract—Fine particles of barium hexaferrite were prepared from aqueous solutions of iron nitrate, barium nitrate and potassium hydroxide by utilizing a continuous flow type supercritical water crystallization method. The influence of stoichiometry (Fe/Ba mole ratio) and alkalinity (R) on the product composition and morphology was studied under fixed temperature, pressure and residence time. Experiments were performed with varying Fe/Ba mole ratios and alkali mole ratio (R). Within mole ratio ranges of $0.5 < Fe/Ba < 5$, $BaO \cdot 6Fe_2O_3$ single phase was produced; and as the Fe/Ba mole ratio increased, α-Fe_2O_3 was also formed and its quantity increased with increasing mole ratio. At an Fe/Ba ratio of 12, stoichiometric mole ratio of $BaO \cdot 6Fe_2O_3$, the only product formed was α-Fe_2O_3 fine particles. In the case of the influence of alkalinity, single phase α-Fe_2O_3 was detected at R of 0.5 and if R exceeded 2, a single phase $BaO \cdot 6Fe_2O_3$ was detected. According to the results of the experiment and the study of reaction mechanisms, the formation of $BaO \cdot 6Fe_2O_3$ proceeds via a non-stoichiometric reaction and the product composition and morphology can be controlled by adjusting the reaction parameters to obtain optimum conditions for $Ba(OH)_2$ precipitate formation.

Key words: Barium Hexaferrite, Supercritical Water Crystallization

INTRODUCTION

Barium hexaferrite ($BaO \cdot 6Fe_2O_3$), which is comprised of hexagonal plate-like particles, has been intensively investigated as a high-density perpendicular magnetic recording medium because of its excellent chemical stability with the direction of magnetization perpendicular to the plane of the plate. In addition, the advantages of reproducibility, oxidation or corrosion resistance, high speed production utilizing existing coating facilities, and the fact that the existing head medium interface is preserved [Chou et al., 1987; Fujiwara, 1985] make this particle a very promising high-density recording medium for next-generation HDTV recording tapes or computer-related storage systems. Particles suitable for high-density magnetic recording should be ultra fine with a narrow size distribution, with good dispersibility in an organic medium [Ataie et al., 1995; Sakai et al., 1992].

Several methods have been proposed to prepare barium hexaferrite fine particles which satisfy these conditions such as glass crystallization [Kubo and Ido, 1982], hydrothermal methods [Sada et al., 1991] and so on. The hydrothermal technique is probably the most attractive one in that it yields an oxide suspension of very fine crystalline metal oxides and a variety of different metal oxides have been synthesized with great success [Wang et al., 1994]. However, this method has poor productivity and the problem of high cost on a large scale due to a long reaction time and batch-wise synthesis by means of an autoclave. As a result of studies aimed at overcoming these problems, the supercritical water crystallization method was proposed [Adschiri et al., 1992].

In supercritical water crystallization, owing to the fact that the metal salt aqueous solution can be heated rapidly to the operating temperature, both hydrolysis and in situ refining of the generated small metal oxide nuclei can occur simultaneously. Thus, high refining rates as well as fast hydrolysis rates can be expected and a flow type continuous process can be developed.

From another point of view, supercritical fluids possess physico-chemical properties such as density, viscosity and diffusivity, which are intermediate between those of liquids and gases. The main interest in supercritical fluids as reaction media relies on their continuously adjustable properties from gas to liquid with small changes of pressure and temperature. Also, for the reactions involving ionic species, the variations of the relative permittivity and ion product influence both the chemical equilibrium and the evolution of the transition state. Supercritical water crystallization is based on homogeneous nucleation and large supersaturation and the particle size is sensitive to decreases with increasing supersaturation. Thus, adjusting the reaction conditions such as pressure, temperature, and concentrations of feed materials may lead to the simultaneous control of size, crystal structure, and morphology of the particle.

This paper describes the preparation and characterization of fine particles of barium hexaferrite by supercritical water crystallization. Among the various variables in supercritical water crystallization, the influence of stoichiometry and alkalinity of the feed materials is studied.

EXPERIMENTAL SECTION

1. Materials

Barium nitrate ($Ba(NO_3)_2$, 98.5%, Junsei Chemical Co., Japan) and iron(III) nitrate ($Fe(NO_3)_3 \cdot 9H_2O$, 98%, Showa Chemical Inc., Japan) precursors were used for barium hexaferrite synthesis without further purification. Feed solutions were prepared for aqueous

†To whom correspondence should be addressed.
E-mail: sdopark@kier.re.kr

mixed solutions of barium nitrate and iron nitrate, dissolved in deionized water (Milli-Q plus, Millipore). The concentration of ferric nitrate was fixed at 0.02 mol// and barium nitrate concentration was varied according to the molar ratio of Fe/Ba. For the purpose of investigating the influence of stoichiometry, the Fe/Ba molar ratio as defined by Eq. (1) was varied from 0.5 to 12.

$$\text{Fe/Ba molar ratio} = \frac{[\text{Fe(NO}_3)_3]}{[\text{Ba(NO}_3)_2]} \tag{1}$$

Potassium hydroxide (KOH, 85%, Duksan, Korea) aqueous solution was used as the base species for adjusting solution pH. Aqueous base solutions were prepared in which the alkali molar ratio was varied from 0.5 to 6, while the volumetric feed rate was the same as that of the Fe/Ba mixed aqueous solution. The alkali molar ratio R, the ratio of KOH concentration to total concentration of nitrate was defined by Eq. (2).

$$\text{Alkali molar ratio} = \frac{[\text{KOH}]}{3[\text{Fe(NO}_3)_3] + 2[\text{Ba(NO}_3)_2]} \tag{2}$$

2. Apparatus and Procedure

Experimental apparatus and procedures used in this work were based on the design of Hakuta et al. [1998]. A schematic diagram of the supercritical water crystallization apparatus used in this work is shown in Fig. 1. The aqueous mixed solution composed of barium nitrate and ferric nitrate, and the base solution composed of KOH, were fed through the degassing unit (Jour Research, X-ActTM) by a non-pulsation high-pressure pump (PUS-11, GL Science Co., Tokyo) at a flow rate of 2 ml/min. These solutions were mixed at the mixing point MP1 at 40 MPa and room temperature. The solution was then heated rapidly to 200 °C at mixing point MP2 by direct mixing with preheated D.I. water fed from another line. After this preheating, the preheated aqueous mixed solution was heated again to the reaction temperature (400 °C) at mixing point MP3 by direct mixing with another preheated water stream. The coil type reactor was made of high-pressure stainless steel (SUS 316) tube with 1/4" external diameter and was 6 m long. The temperatures of the mixing point and the reactor were measured by K-type thermocouples that were located at each mixing point and at the inlet and outlet points of the reactor. The temperatures of the reactor and preheaters were kept constant by an external electric furnace with a PID

Fig. 1. Schematic diagram of apparatus.

temperature controller, and the temperature distribution was uniform within ±1 °K. Thermocouples and the temperature controller were calibrated by utilizing a signal generator (Model 6500, GLA electronica).

The volumetric flow rates of the preheated water streams were adjusted to set the residence time in the reactor and between MP2 and MP3 at 80 sec and 6 sec, respectively. Residence time was calculated by Eq. (3).

$$\tau = \frac{V}{R} \cdot \frac{\rho}{\rho_F} \tag{3}$$

Where, F is the total flow rate of solution evaluated at ambient pressure and temperature and V is the volume of the reactor or volume of the tube between MP2 and MP3. Also, ρ is the density of solution at experimental pressure and temperature, and ρ_F is the solution density at ambient pressure and temperature. The density of the solution was assumed to be the same as pure water density and was taken from steam tables because the concentrations of precursors were very low. At the outlet of the reactor, rapid cooling utilizing a double-pipe type heat exchanger was performed to prevent the formation of hydroxide products at around 150 °C. Product particles were collected in a 0.5 μm in-line filter and filtrate was vented through the back pressure regulator (Model 26-1722-24, TESCOM) which was also used for controlling the pressure of the total system.

3. Characterization

Prepared sample powders were washed with D.I. water several times and dried at around 60 °C in a drying oven. Afterward, the composition of synthesized samples was determined by X-ray diffraction (XRD, Rigaku, 30 kV-25 mA) by using CuKα radiation with a scan rate of 2θ/min. Particle size and morphology of the obtained particles were observed by utilizing scanning electron microscopy (SEM, Philips, XL-30).

RESULTS AND DISCUSSION

1. Reproducibility Test

Reproducibility tests were performed to confirm the reliability of the instrument and the experimental procedure used in this work. The system design consisted of three mixing points. Aqueous mixed solutions of Fe/Ba and KOH were mixed at MP1 at 40 MPa and room temperature. At mixing point MP1, hydrolysis reactions of $\text{Fe(NO}_3)_3$ and $\text{Ba(NO}_3)_2$ occurred and transitions to Fe(OH)_3 and Ba(OH)_2 proceeded. The temperature of the mixed solution was elevated to 200 °C by direct mixing with preheated water at mixing point MP2. In an alkali medium, the precipitated Fe(OH)_3 is transformed into α-FeOOH or α-Fe_2O_3, or a mixture of the two, depending on the temperature and residence time [Nam et al., 1999]. Also, precipitation of Ba(OH)_2 tends to be initiated because of the decrease in solubility owing to the increase in temperature. It is noted that the formation of agglomerates influences the final product particle composition and morphology. If the temperature at MP2 exceeded 300 °C or the residence time was long enough (about 25 sec), hematite (α-Fe_2O_3) as well as BaO·6Fe_2O_3 or just a single phase of hematite was formed. Because α-Fe_2O_3 is chemically stable, translation of α-Fe_2O_3 to BaO·6Fe_2O_3 by reaction with Ba(OH)_2 takes a long reaction time. So, in order for BaO·6Fe_2O_3 to be produced con-

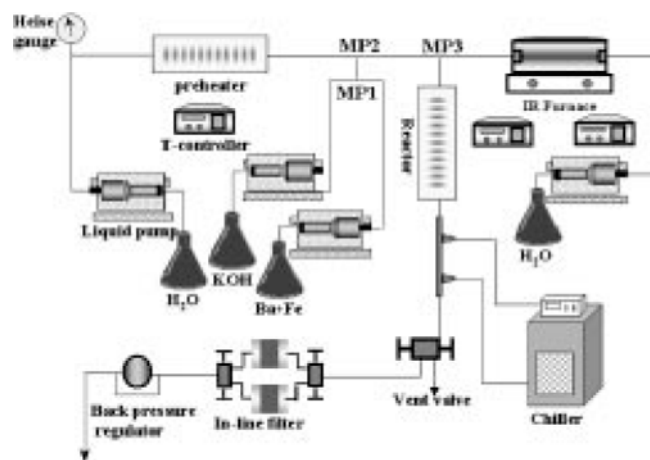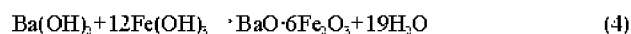tinuously in a short reaction time, the reaction must be carried out at a temperature below 300 °C. On the other hand, if the temperature of MP2 was lower than 200 °C, final product particles were single phase of $BaO \cdot 6Fe_2O_3$, but large particles were produced. Therefore, MP2 temperature and residence time should be determined with care. The influence of MP2 temperature and residence time on the final product compositions and morphology was illustrated in previous work [Kiyama, 1976].

At mixing point MP3, the temperature of the solution was elevated to 400 °C and solutions were raised to the supercritical water condition by direct mixing with preheated water from another line. At this point, nucleation by chemical bonding between α-FeOOH and $Ba(OH)_2$, dehydration reactions and crystal growth by inclusion of nuclei proceeded. In a supercritical water medium, because diffusion coefficients are extremely higher than in a commercial hydrothermal process, dehydration reaction followed by chemical bonding occur simultaneously. Also, the decrease of the solvating power decreases the solubility and increases the supersaturation. Supercritical water crystallization is based on homogeneous nucleation and large supersaturation in a supercritical solvent, which leads to production of powders consisting of ultra fine particles with a narrow distribution range.

Reproducibility tests were performed four times at same conditions of Fe/Ba=2 and alkali mole ratio R=4. Powder X-ray diffraction patterns showed the formation of single-phase hexagonal plate-like particles of barium hexaferrite. SEM photographs of the product showed that the products consist of very small particles with no remarkable size difference and a narrow range size distribution as shown in Fig. 2. Both XRD patterns and SEM photograph confirmed the consistency in each case.

2. Influence of Fe/Ba Molar Ratio

In a wet chemical process such as a hydrothermal process or supercritical crystallization for $BaO \cdot 6Fe_2O_3$ formation, the reaction can be written stoichiometrically as Eq. (4).

$$Ba(OH)_2 + 12Fe(OH)_3 \rightarrow BaO \cdot 6Fe_2O_3 + 19H_2O \qquad (4)$$

However, it is known that reaction of ferric hydroxide with an excess stoichiometry of barium hydroxide yields ultra fine particles of barium hexaferrite, whereas the stoichiometric reaction produces a single phase of α-Fe$_2$O$_3$. Thus, the influence of stoichiometry on the particle compositions and morphology was examined by varying the Fe/Ba molar ratio. For characterizing the influence of stoichiometry, the alkali molar ratio was fixed at 4. It was assumed that there was no influence due to alkali molar ratio because the pH of the outlet effluent in each case was approximately 12.4.

Fig. 3 shows XRD patterns of product synthesized by supercritical water crystallization as a function of Fe/Ba molar ratio. As shown in Fig. 3 the particles were proven to be a single phase of $BaO \cdot 6Fe_2O_3$ in the range of 0.5<Fe/Ba<5, although a trace amount of α-Fe$_2$O$_3$ was formed when the Fe/Ba molar ratio was 5. With increasing Fe/Ba molar ratio, the amount of α-Fe$_2$O$_3$ phase increases and when the stoichiometric reaction was reached (Fe/Ba=12), α-Fe$_2$O$_3$ became the predominant phase at the expense of $BaO \cdot 6Fe_2O_3$. Fig. 3 also depicts that as the Fe/Ba molar ratio increased, an increasing amount of α-Fe$_2$O$_3$ was produced along with $BaO \cdot 6Fe_2O_3$ phase in the mixture. As the Fe/Ba molar ratio reached stoichiometry at 12, a very small amount of $BaO \cdot 6Fe_2O_3$ in addition to α-Fe$_2$O$_3$ was found in the obtained product. Sometimes $BaCO_3$ was also detected, and this was probably due to carbonation of excess Ba with atmospheric CO_2 in the drying step. However, it could easily be removed by wash-
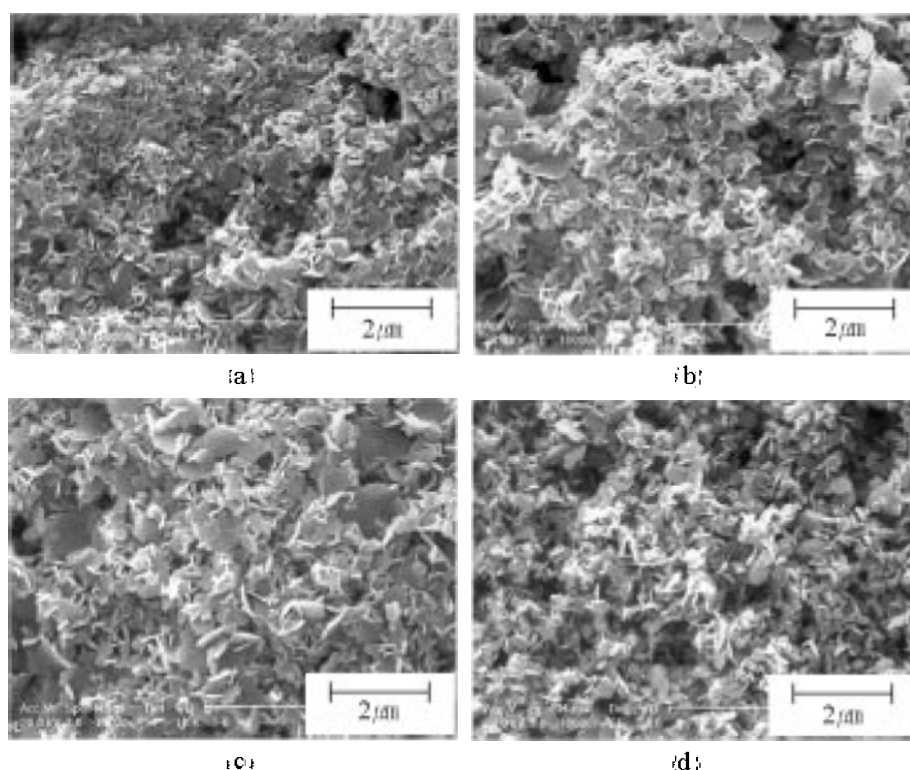

(a)

(b)

(c)

(d)

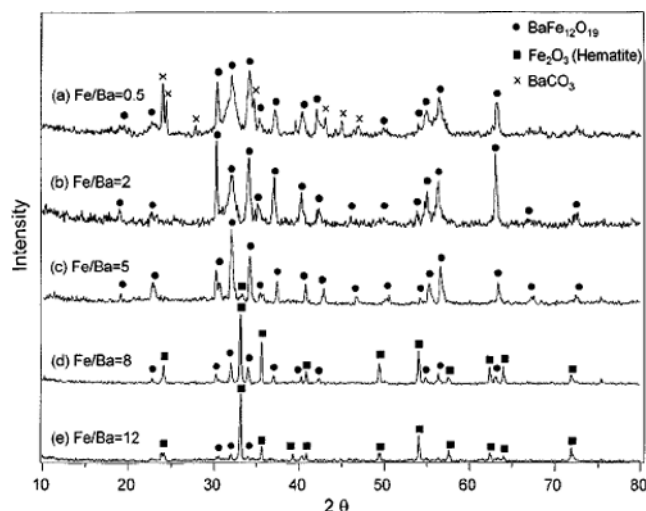**Fig. 2. SEM photographs to demonstrate reproducibility.**

Fig. 3. XRD patterns with various Fe/Ba ratios at R=4.

ing with dilute HCl (35%) solution. To illustrate this phenomenon, XRD results without acid washing were used in the case of a Fe/Ba molar ratio of 0.5.

In the present work, intermediate products such as $BaO \cdot Fe_2O_3$ according to Ataie et al. [1995] or $BaO \cdot 4.5Fe_2O_3$ as reported by Kiyama [1976] were not observed. The cause for this is believed to be that in the hydrothermal method used by previous researchers, the solution temperature was raised at 4-5 °C/min, allowing metastable intermediates to form at various temperatures. But in the supercritical water crystallization technique used in this work, dramatic heating is achieved by direct mixing between feed material and preheated water.

Next, the effect of the molar ratio of Fe/Ba on the mean particle size was also investigated. Fig. 4 shows SEM photographs that imply that the mean particle size varies with Fe/Ba molar ratio. For powder derived at Fe/Ba molar ratio of 0.5, agglomerates of ultra fine particles, which have only a low crystallinity, are formed, though the XRD patterns appear to be $BaO \cdot 6Fe_2O_3$. At Fe/Ba molar ratio of 2, barium hexaferrite crystals with thin hexagonal plate morphology and sizes between 0.1-0.2 μm are formed. Also, the result of SEM analysis demonstrates the fact that the particle size increases with increasing Fe/Ba molar ratio, with the particle size of

produced barium hexaferrite becoming 0.5 μm at Fe/Ba molar ratio of 5.

From the XRD and SEM results, it can be seen that both the phase composition and the particle size of the samples synthesized by supercritical water crystallization are a strong function of Fe/Ba molar ratio, whereas the size distribution and particle shape are not. Reasons why the product composition and particle size changes with variations of Fe/Ba molar ratio can be derived from the reaction mechanisms and the activity of the Ba compounds. As mentioned earlier, $BaO \cdot 6Fe_2O_3$ formation is carried out as a result of chemical bonding and dehydration reaction between α-FeOOH and $(BaOH)_2$. By increasing the Ba concentration, not only activity but also reactivity of Ba compounds is increased. It is therefore believed that as the Fe/Ba molar ratio decreases (i.e., Ba concentration increases), chemical bonding between $(BaOH)_2$ and α-FeOOH tends to take place more easily, and the number of host nuclei increases. The size of synthesized particles is very sensitive to the degree of supersaturation: the higher the supersaturation, the smaller the particles. Correspondingly, the mean particle size decreases with decreasing Fe/Ba molar ratio. On the other hand, because reactivity of Ba composition decreases as the Fe/Ba molar ratio increases, the formation of α-Fe$_2O_3$ by chemical bonding and dehydration between α-FeOOH occurs predominantly. In that case, Ba compounds may be present in the neighborhood, but are probably not in a position to contribute to the chemical structure.

In the wet chemical method, the dehydration reaction of α-FeOOH to form α-Fe$_2O_3$ at temperatures above 300 °C occurs very quickly. So, since the dehydration reaction of α-FeOOH and the chemical bonding reaction with the Ba compounds proceed competitively, a non-stoichiometric reaction occurs. Such a non-stoichiometric reaction cannot be obtained by other methods such as the usual ceramic method and the glass crystallization method; therefore, it is a characteristic of liquid phase synthesis.

3. Influence of Alkali Molar Ratio (R)

The alkali molar ratio was varied from 0.5 to 6 to investigate its effect on the phase formation, particle size and size distribution of the product, while the Fe/Ba molar ratio was kept fixed at 2. Fig. 5 compares the XRD patterns of product synthesized at alkali molar ratios of 0.5, 2, 4 and 6, respectively. A single phase of α-Fe$_2O_3$ was detected at the alkali molar ratio of 0.5 that was low concentration of KOH for substituting the total nitrate to hydroxide. When

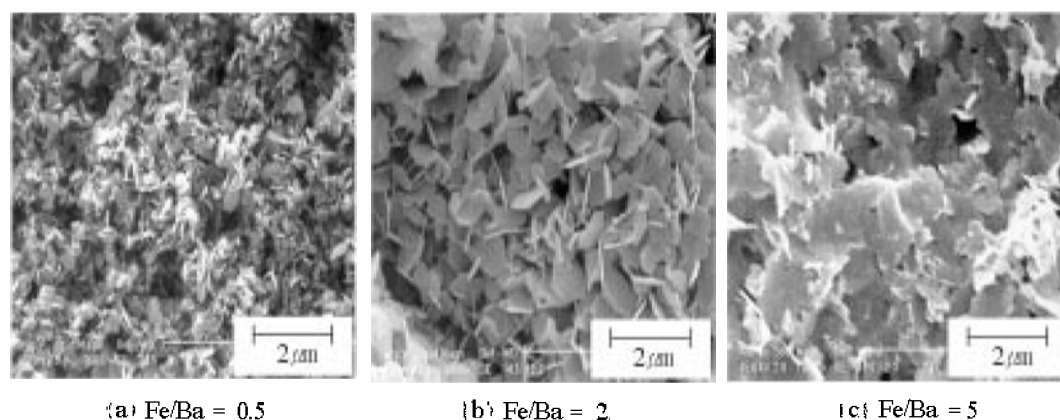(a) Fe/Ba = 0.5   (b) Fe/Ba = 2   (c) Fe/Ba = 5
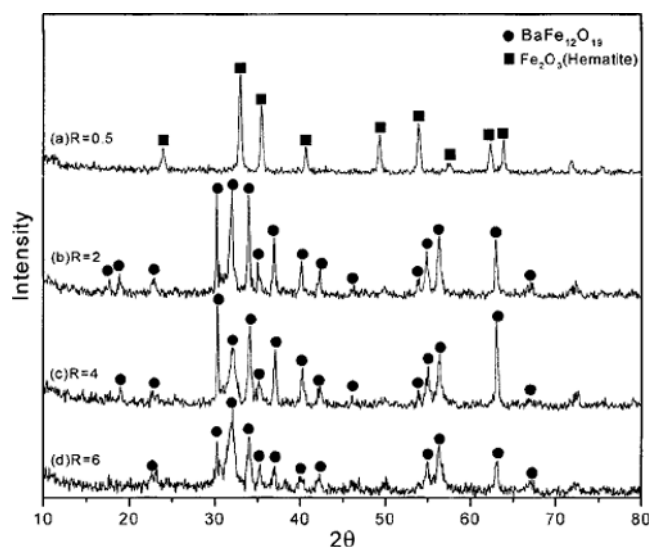
Fig. 4. SEM micrographs with various Fe/Ba ratios at R=4.

Fig. 5. XRD patterns with various R ratio at Fe/Ba=2.

the alkali molar ratio was increased to 2, the only XRD detectable phase was $BaO \cdot 6Fe_2O_3$. It also can be seen that alkali molar ratios of 4 and 6 resulted in the formation of single phase of $BaO \cdot 6Fe_2O_3$. The phenomena of composition variation of the final product can be illustrated by considering the formation of precipitates of $Ba(OH)_2$. Thus, when $BaO \cdot 6Fe_2O_3$ was synthesized from chemical bonding with α-FeOOH and dehydration $Ba(OH)_2$ is formed. However when α-Fe$_2$O$_3$ was synthesized by chemical bonding between α-FeOOH and dehydration $Ba(OH)_2$ was not formed. This agrees with the result of general hydrothermal synthesis. In the hydrothermal method, because $Ba(OH)_2$ is sufficiently soluble in water, precipitation of $Ba(OH)_2$ initiates above pH 11. On the other hand, according to Kiyama [1976], when the alkali molar ratio was 0.8, the pH of the resulting suspension became 2.4-2.8, and most of the Fe^{3+} ions were precipitated. And after autoclaving, it turned out that pH<11 for the suspensions. In this experiment, the pH of the outlet effluent was 3.1. This means that formation of $Ba(OH)^+$ does not occur while Fe^{3+} is completely precipitated at these pH range. When alkali molar ratio exceeds 2, pH of the outlet fluent is extremely elevated to over 12 and $BaO \cdot 6Fe_2O_3$ can be synthesized as a result of the formation of $Ba(OH)^+$.

The alkali molar ratio also affects the particle size and size distribution of barium hexaferrite powder. Fig. 6 shows a scanning electron micrograph with the uniform size of the hexagonal plate-like particles of barium hexaferrite particles synthesized in various alkali molar ratios. The mean particle size is shown to decrease with increasing alkali molar ratio, though their crystallinity also decreases. The powders derived at alkali molar ratio of 2 and 4 consist of hexagonal plates of barium hexaferrite that are well dispersed. At an alkali molar ratio of 6, the barium ferrite particles become less regular in particle shape and form particle agglomerates. The reasons why the particle size decreases with increasing alkali molar ratio can also be illustrated from the degree of $Ba(OH)_2$ precipitate formation. Because the solubility of $Ba(OH)_2$ decreases with increasing solution pH, the number of $Ba(OH)_2$ precipitates in the reactor increases, so the number of $BaO \cdot 6Fe_2O_3$ crystal nuclei synthesized from chemical bonding with α-FeOOH also increases and particle size decreases. Although it is not certain from this work, Ataie et al. [1995] suggested that surface charge density of barium hydroxide and iron oxide particles and the electrostatic potential between them, and their tendency to form barium hexaferrite are strong function of the solution pH [Ataie et al., 1995]. Hence, any change in the surface charge characteristics of the particles is likely to result in changes in the phase composition, thermal behavior, particle morphology, particle agglomeration behavior, and magnetic properties of the samples. From the results of the influence of alkalinity study, product composition did not vary with alkali molar ratio in the presence of excess KOH, but the particle size and morphology is a strong function of alkalinity.

Additionally in the present work, it can be shown the difference in the particle size and morphology of produced α-Fe$_2$O$_3$ is caused by the formation of $Ba(OH)_2$ precipitates. Fig. 7(a) shows an SEM photograph of α-Fe$_2$O$_3$ produced at Fe/Ba=2 and R=0.5, and Fig. 7(b) and Fig. 7(c) show α-Fe$_2$O$_3$ produced at Fe/Ba=8 and 12 and R=4, respectively. As mentioned earlier, the former is a case where $Ba(OH)_2$ did not precipitate and the latter is a case where $Ba(OH)_2$ precipitated but no reaction occurred owing to low reactivity. From the SEM photographs, it can be seen that hexagonal plate type particles with relatively larger size were obtained in the case where $Ba(OH)_2$ was formed, whereas spherical ultra fine particles were obtained in the case where $Ba(OH)_2$ was not formed. It is believed that the Ba compound in solution plays a role as an agent for en-

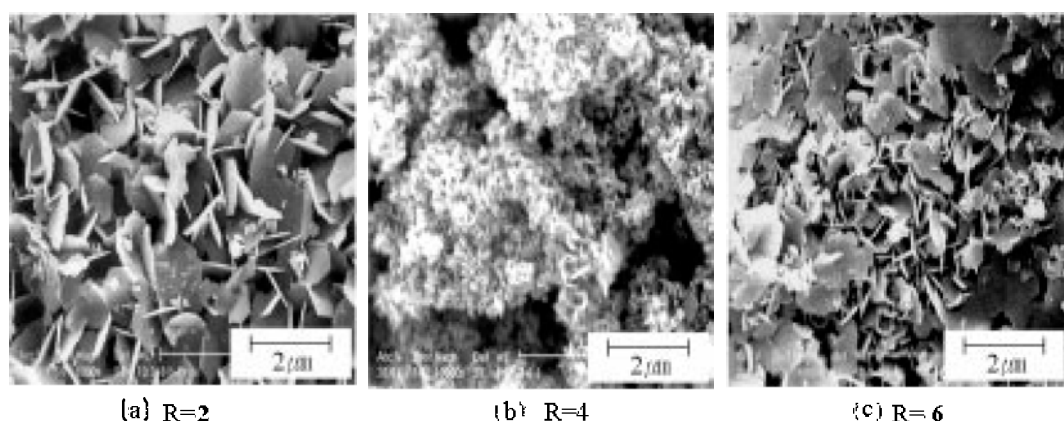(a) R=2   (b) R=4   (c) R=6

Fig. 6. SEM micrograph with various R ratios at Fe/Ba=2.

(a) **Fe/Ba= 4**
R = 0.5
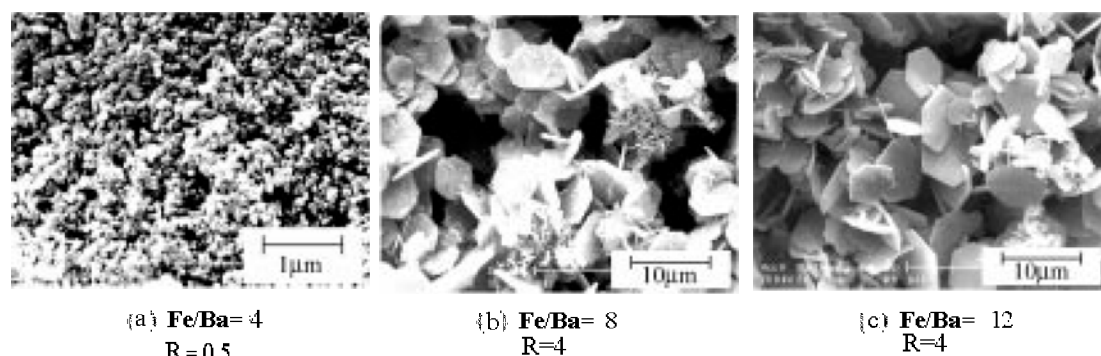
(b) **Fe/Ba= 8**
R=4

(c) **Fe/Ba= 12**
R=4

Fig. 7. α-F_2O_3 morphology changes with synthetic conditions.

hancing crystal growth and controls the favorable growth of a particular crystal face.

CONCLUSION

The influence of stoichiometry and alkalinity on the composition and morphology of barium hexaferrite particles synthesized by the supercritical water crystallization method were studied. In this preparation technique, fine particles with narrow size distribution can be easily obtained. Furthermore, it can be shown that non-stoichiometric substitution can be attained. Composition and morphology of produced particles are strong functions of both Fe/Ba molar ratio and alkalinity. Particle size decreases with decreasing Fe/Ba molar ratio, and with increasing alkali molar ratio. This is probably because of the influence of supersaturation followed by an increase in nuclei formation owing to the degree of $Ba(OH)_2$ precipitation. Thus, it is concluded that the product composition and morphology can be controlled by adjusting the reaction conditions to obtain optimum conditions of $Ba(OH)_2$ precipitate formation.

ACKNOWLEDGEMENT

NOMENCLATURE

F   : flow rate [cm^3/sec]
Fe/Ba   : molar ratio of ferric nitrate to barium nitrate
R   : alkali molar ratio
V   : reactor volume [cm^3]

Greek Letters
ρ : density of water in reactor [g/cm^3]
τ : residence time [sec]

REFERENCES

Adschiri, T., Kanazawa, K. and Arai, K., "Rapid and Continuous Hydrothermal Crystallization of Metal Oxide Particles in Supercritical Water," *J. Am. Ceram. Soc.*, **75**, 1019 (1992).

Ataie, A., Piramoon, M. R., Harris, I. R. and Ponton, C. B., "Effect of Hydrothermal Synthesis Environment of the Particle Morphology, Chemistry, and Magnetic Properties of Barium Hexaferrite," *J. Mater. Sci.*, **30**, 5600 (1995).

Chou, F., Feng, X., Li, J. and Liu, Y., "Magnetic Properties of $BaFe_{12-2x}Co_xTi_xO_{19}$ Fine Particles Prepared by Coprecipitation Tempering," *J. Appl. Phys.*, **61**(8), 3881 (1987).

Fujiwara, T., "Barium Ferrite Media for Perpendicular Recording," *IEEE Trans. Magn.*, Mag-**21**(5), 1480 (1985).

Hakuta, Y., Adschiri, T., Suzuki, T., Chida, T., Seino, K. and Arai, K., "Flow Method for Rapid Producing Barium Hexaferrite Particles in Supercritical Water," *J. Am. Ceram. Soc.*, **81**(9), 2461 (1998).

Kiyama, M., "Conditions for the Formation of Compounds Consisting of BaO and Fe_2O_3 from Aqueous Suspensions," *Bull. Chem. Soc. Jpn.*, **49**(7), 1855 (1976).

Kubo, O., Ido, T. and Yokoyama, H., "Properties of Ba Ferrite Particles for Perpendicular Magnetic Recording Media," *IEEE Trans. Magn.*, Mag-**18**(5), 1122 (1982).

Nam, S. C., Lee, J. H., Kim, J. G., Kim, K. J. and Park, S. D., "Continuous Synthesis of Barium Hexaferrite Particles by Supercritical Water Crystallization - Effect of Temperature/Pressure at Mixing Point," *Theo. Appl. Chem. Eng.*, **5**(2), 4149 (1999).

Sada, E., Kumazawa, H. and Cho, H. M., "Synthesis of Barium Ferrite Ultrafine Particles by a Hydrothermal Method," *Ind. Eng. Chem. Res.*, **30**(6), 1319 (1991).

Sakai, H., Hanawa, K. and Aoyagi, K., "Preparation and Magnetic Properties of Barium Ferrite Fine Particles by the Coprecipitation Salt-Catalysis Method," *IEEE Trans. Magn.*, **28**(6), 3355 (1992).

Wang, M. L., Shih, Z. W. and Lin, C. H., "Reaction of α-Fe_2O_3 with $Ba(OH)_2$ under Hydrothermal Conditions," *J. Cryst. Growth.*, **139**, 47 (1994).